CFD Letters

Journal homepage:
https://semarakilmu.com.my/journals/index.php/CFD_Letters/index
ISSN: 2180-1363

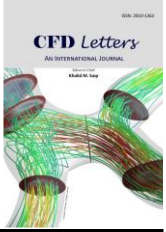

Effects of Mesh Number and the Time-step-based Parameter on the Accuracy of Couette Solution

Ladyn Zulkapri[1], Aslam Abdullah[1,*], Ahmad Hamdan Ariffin[1]

[1] Department of Aeronautical Engineering, Faculty of Mechanical and Manufacturing Engineering, Universiti Tun Hussein Onn Malaysia, 86400 Parit Raja, Johor, Malaysia

ARTICLE INFO

Article history:
Received 4 January 2024
Received in revised form 6 February 2024
Accepted 10 March 2024
Available online 31 August 2024

Keywords:
Couette solution; Crank-Nicolson method; the time-step-based parameter; convection-diffusion

ABSTRACT

Couette flow, a flow between two parallel plates with one plate in motion and the other stationary, has been extensively studied and applied in various engineering and scientific fields. However, optimizing the accuracy of numerical solutions for such a flow is always a challenge. In this study, we focus on a quasi-1-dimensional Couette flow to investigate the impact of mesh number and the time-step-based parameter on the accuracy of the numerical solution. The Crank-Nicolson finite difference method is employed to solve the corresponding equation. The results suggest that the error linked to the unsteady Couette solution increases as the number of intervals rises. However, increasing the time-step-based parameter, has the potential to reduce the error, although it may lead to a simultaneous increase in the likelihood of oscillation. The findings can be leveraged in real applications to enhance the accuracy, efficiency, and reliability of computational simulations for improving the quality of the results, making informed decisions, and advancing the state of the art in respective fields.

1. Introduction
1.1 Engineering and Science Applications

Couette flow has been studied extensively in recent years. It is a type of flow between two parallel plates, where one plate is moving and the other is stationary. It has been used in various applications such as fluid transport devices, MHD power generators, and directional solidification.

One of the most prominent applications of Couette flow in the manufacturing industry is the extrusion process. The gap between the barrel and the screw of the extruder is narrow such that assuming a fluid flowing between parallel plates leads to representative of results. The findings are significant in increasing the production rate and enhancing the quality of the final product [1].

Couette flow is also considered to represent the flow in plain bearings which are used in many industries and across various applications where there is a need to cost-efficiently and reliably meet the challenge of oscillating movements and any possible misalignments [2].

* *Corresponding author.*
E-mail address: aslam@uthm.edu.my (Aslam Abdullah)

https://doi.org/10.37934/cfdl.17.1.3545

One study characterizes near-wall turbulence in the buffer region of Couette and Poiseuille flows in terms of nonlinear three-dimensional solutions to the incompressible Navier-Stokes equations for wall-bounded shear flows [3]. Another study presents an extensive compilation of direct numerical simulation (DNS) data for Poiseuille and Couette flows, from the laminar into the fully turbulent regime, with the goal of highlighting similarities and differences [4]. The data suggest that, for a given bulk velocity, Couette flow yields less resistance than Poiseuille flow and greater turbulence kinetic energy, which may be beneficial for more efficient diffusion.

Couette flow has also been studied in the context of stability analysis. One study investigates the linear stability of viscous compressible plane Couette flow for a perfect gas governed by Sutherland viscosity law [5]. Another study examines the stability of plane Couette flow of a Newtonian liquid with constant viscosity and variable density subjected to a temperature gradient [6].

Couette flow has also been used in the study of turbulence. Experiments and numerical simulations have shown that turbulence in transitional wall-bounded shear flows frequently takes the form of long oblique bands if the domains are sufficiently large to accommodate them. These turbulent bands have been observed in plane Couette flow, plane Poiseuille flow, counter-rotating Taylor–Couette flow, torsional Couette flow, and annular pipe flow [7].

In addition, Couette flow has been used in the study of heat transfer. One study presents analytical analysis of the steady flow of an incompressible third grade fluid between two parallel plates, and the effect of heat transfer is considered [8].

Overall, Couette flow plays an important role in various engineering and science applications and has been studied extensively in recent years. Its applications range from fluid transport devices to MHD power generators and directional solidification. The application of Couette flow is summarized in Table 1.

Table 1
The review summary of Coutte flow application

No	Application	References
1	The extrusion process in manufacturing industry	[1]
2	Oscillating movements and any possible misalignments in plain bearings	[2]
3	Characterization of near-wall turbulence in the buffer region	[3,4]
4	Flow stability analysis	[5,6]
5	Turbulence flow analysis	[7]
6	Heat transfer flow analysis	[8]

There are relationships between Couette flow and other flows. For instance, its connection to convection-diffusion flow has been studied by several researchers [4,9,10]. Domaradzki and Metcalfe [9] suggested that Couette flow can enhance heat transfer and may be beneficial for more efficient diffusion. Shear tends to organize the flow into quasi-two-dimensional rolls parallel to the mean flow and can enhance heat transfer, while at higher Rayleigh number, shear tends to disrupt the formation of convective plumes and can reduce heat transfer.

1.2 Numerical Methods for Parabolic Equations

Parabolic equations are a class of partial differential equations that arise in many fields of science and engineering. Implicit finite difference methods are commonly used to solve these equations including the Couette equation numerically.

Dawson, Du, and Dupont [11] proposed a finite difference domain decomposition algorithm for the numerical solution of the heat equation. This algorithm can be applied to parabolic equations, giving domain decomposition iterative methods for the solution of the equations at each time step. Another approach has also been given [11], which uses overlapping subdomains to approximately solve the implicit equations arising from a standard finite difference discretization.

Kuznik and Virgone [12] used a finite-difference method to solve numerically the problem of wallboard containing phase change material. They replaced the continuous information contained in the exact solution of the differential equation with discrete temperature values.

Olshanskii, Reusken, and Xu [13] studied numerical methods for the solution of partial differential equations on evolving surfaces. They derived and analyzed a variational formulation for a class of diffusion problems on the space-time manifold.

Lord and Tambue [14] considered the numerical approximation of a general second-order semi-linear parabolic stochastic partial differential equation (SPDE) driven by additive space-time noise. They introduced a new modified scheme using a linear functional of the noise with a semi-implicit Euler-Maruyama method in time and in space.

Liu [15] presented a stable explicit difference approximation to parabolic partial differential equations. The method is a modification of the method of Douglas and Rachford, which achieves the higher-order accuracy of a Crank-Nicholson formulation while preserving the advantages of the Douglas-Rachford method: unconditional stability and simplicity of solving the equations at each time level.

Crank-Nicolson scheme is a finite difference scheme used to solve parabolic partial differential equations. The scheme is almost unconditionally stable and converges optimally [16]. It is more stable than fully explicit methods and without the damping effects of fully implicit methods [17]. The scheme has been used to solve various problems [18, 19], including the Schrödinger equation [20], the Huxely equation [21], and the time fractional Sobolev equations [22]. The scheme has also been used in combination with other methods, such as the finite element method [21] and the finite volume element method [22].

In conclusion, implicit finite difference methods are widely used to solve parabolic equations including Couette equation numerically. In this study, we use Crank-Nicolson scheme which is a well-known method for solving Couette equation [16]. The scheme has been shown to be accurate and efficient in solving various problems, and it is still a well-accepted method in the scientific community. In numerical method, the selection of mesh number and the time-step based parameter is crucial to obtain an accurate and less error output. However, these parameters are different for any application. Therefore, the objective of this research is to study the effects of mesh number and the time-step-based parameter on the accuracy of Coutte flow.

2. Methodology

The governing equation is expressed by

$$\rho \partial_t u = \mu {\partial_y}^2 u \tag{1}$$

Where ρ is density, u is x-component of velocity field, μ is viscosity, and the flow variables are independent of x and y-component of velocity field $v = 0$. This unsteady x-momentum equation for incompressible Couette flow is a parabolic partial differential equation for which a time-marching solution represents a well-posed problem.

Corresponding dimensionless variables are defined as

$$u^* = u/u_Y \qquad y^* = y/Y \qquad t^* = tu_Y/Y \tag{2}$$

Thus, Eq. (1) can be written in dimensionless form as

$$\rho\, u_Y^2/Y\, \partial_{(tu_Y/Y)}(u/u_Y) = \mu\, u_Y/Y^2\, \partial^2_{\left(\frac{y}{Y}\right)}(u/u_Y) \tag{3}$$

or

$$\partial_{t^*}u^* = 1/\mathrm{Re}_Y\, \partial^2{}_{y^*}u^* \tag{4}$$

Where Re_Y is the Reynolds number based on the height of the top plate from the bottom one, Y. The steady state solution is given by

$$u^* = y^* \tag{5}$$

We use Crank-Nicolson method to solve Eq. (4) numerically [1, 23]. Assuming that the velocity profile is non-linear, the initial conditions are

$$u^* = 0 \text{ at } y^* = [0, Y) \tag{6}$$

and

$$u^* = u_Y \text{ at } y^* = Y \tag{7}$$

while the boundary conditions are

$$u^* = 0 \text{ at } y^* = 0 \tag{8}$$

and

$$u^* = u_Y \text{ at } y^* = Y \tag{9}$$

By setting up a time marching solution for the flow field beginning with the initial conditions, the velocity profile is expected to change in steps of time until it reaches the steady state.

The solution of Eq. (4) is performed on a uniform mesh. The vertical distance, Y across the duct is divided into N equal increments of length Δy by distributing $N+1$ mesh points over Y as

$$\Delta y = Y/N \tag{10}$$

The time-step-based parameter E is defined as

$$E = \frac{\Delta t^*}{\mathrm{Re}_Y(\Delta y^*)^2} \tag{11}$$

The error corresponding to each mesh number is defined as

$$Error = \frac{\Sigma / u^* - u^*_{exact} /}{N+1} \quad (12)$$

The error percentage is given by

$$Error\% = \frac{\Sigma |u^* - u^*_{exact}|}{\Sigma u^*_{exact}} \times 100\% \quad (13)$$

The average error percentage can then be calculated as

$$Error\%_{av} = \frac{\Sigma Error\%}{4} \quad (14)$$

3. Results

3.1 Preliminary Results

The initial number of intervals N is 20. The parameter N is then increased by a factor 2 until it subsequently reaches 5120. The initial findings are shown in Figure 1 and Figure 2 for 40 time steps. In Figure 1 where N ranges from 20 to 320, the corresponding velocity profiles oscillate. For N ranges from 640 to 5120, the velocity profiles leave that of steady state from the very beginning. Oscillations occur when y^* approaches 1. Thus, both figures present physically unacceptable results.

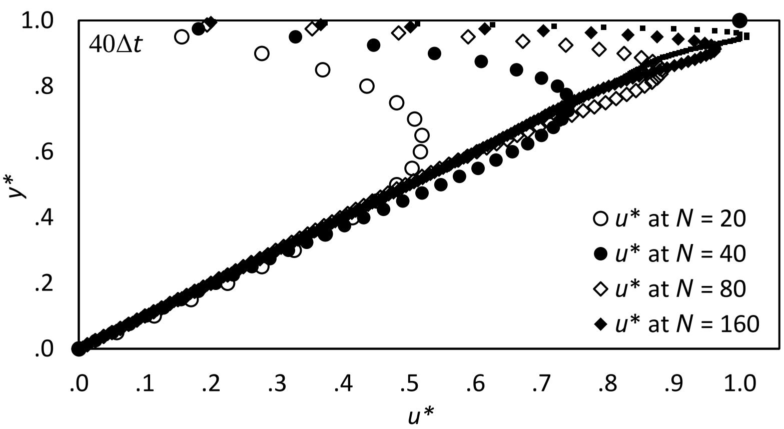

Fig. 1. Velocity profile, u^* against vertical distance, y^* at $40\Delta t$ for a specific range of the number of intervals N from 20 to 320

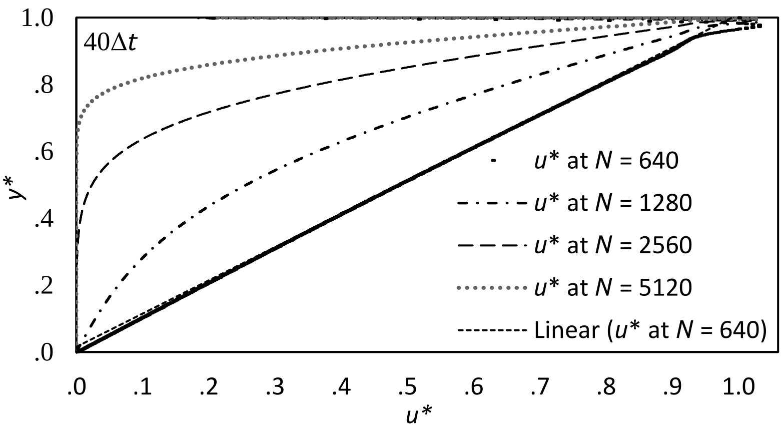

Fig. 2. Velocity profile, u^* against vertical distance, y^* at $40\Delta t$ for a specific range of the number of intervals N from 640 to 5120

3.2 Main Results
3.2.1 Case I: simulation results after 100 time steps

As tabulated in Table 2, $Error$ displays an upward trend for each E except for $E \geq 25$. In addition, $Error\%$ increases with respect to N except for $E \geq 25$. There is an early sign of oscillation when both $Error$ and $Error\%$ fluctuate for $E = 25$. Data in Table 2 also indicates that the higher the time-step-based parameter, E, the higher the tendency of velocity profile to oscillate.

Average error percentage, $Error\%_{av}$ shows initially a downward trend with respect to E. However, for $E \geq 50$, the data is invalid due to the oscillations.

Table 2
Data corresponding to the time-step-based parameter, E and the number of mesh intervals, N after 100 time steps

E	N	Oscillation	$Error$	$Error\%$	$Error\%_{av}$
1	20	NO	0.03272	6.545	51.363
	40	NO	0.21338	42.677	
	80	NO	0.35430	70.879	
	160	NO	0.42677	85.353	
3.125	20	NO	0	0.001	33.911
	40	NO	0.05754	11.508	
	80	NO	0.24762	49.538	
	160	NO	0.37298	74.596	
6.25	20	NO	0	0	24.131
	40	NO	0.00833	1.666	
	80	NO	0.15257	30.522	
	160	NO	0.32167	64.335	
10	20	NO	0	0	18.083
	40	NO	0.00078	0.156	
	80	NO	0.08555	17.115	
	160	NO	0.27531	55.062	
12.5	20	NO	0	0	15.374
	40	NO	0	0.001	
	80	NO	0.05812	11.626	
	160	NO	0.24934	49.867	
25	20	NO	0.00014	0.029	8.109
	40	NO	0.00007	0.015	
	80	NO	0.00831	1.662	
	160	NO	0.15364	30.729	
50	20	NO	0.00119	0.238	3.046
	40	NO	0.00061	0.122	
	80	YES	0.00040	0.080	
	160	YES	0.05872	11.745	
100	20	YES	0.00500	1.000	0.909
	40	YES	0.00256	0.512	
	80	YES	0.00147	0.294	
	160	YES	0.00916	1.831	

3.2.2 Case II: simulation results after 200 time steps

Data in Table 3 indicate that $Error$ increases for each E except for $E \geq 50$. Moreover, $Error\%$ displays an upward trend with respect to N except for $E \geq 50$. Fluctuations in both $Error$ and $Error\%$ for $E = 50$ indicate an early sign of oscillation. It is obvious that the tendency of velocity profile to oscillate is higher with E.

Initially downward trend of $Error\%_{av}$ with respect to E can be observed. For $E \geq 100$, however, the oscillations invalidate the data.

Table 3
Data corresponding to the time-step-based parameter, E and the number of mesh intervals, N after 200 time steps

E	N	Oscillation	*Error*	*Error%*	$Error\%_{av}$
1	20	NO	0.00281	0.563	40.618
	40	NO	0.11507	23.014	
	80	NO	0.29665	59.345	
	160	NO	0.39776	79.551	
3.125	20	NO	0	0	24.131
	40	NO	0.00833	1.666	
	80	NO	0.15257	30.522	
	160	NO	0.32167	64.335	
6.25	20	NO	0	0	15.372
	40	NO	0	0.001	
	80	NO	0.05810	11.624	
	160	NO	0.24933	49.865	
10	20	NO	0	0	10.228
	40	NO	0	0	
	80	NO	0.01824	3.650	
	160	NO	0.18632	37.264	
12.5	20	NO	0	0	8.098
	40	NO	0	0	
	80	NO	0.00831	1.662	
	160	NO	0.15364	30.729	
25	20	NO	0	0	2.936
	40	NO	0	0	
	80	NO	0.00009	0.018	
	160	NO	0.05863	11.725	
50	20	NO	0.00014	0.029	0.444
	40	NO	0.00007	0.015	
	80	NO	0.00011	0.022	
	160	NO	0.00855	1.711	
100	20	NO	0.15144	30.288	7.641
	40	NO	0.00061	0.122	
	80	YES	0.00042	0.084	
	160	YES	0.00036	0.072	

3.2.3 Case III: simulation results after 400 time steps

Increment of $Error$ and $Error\%$ with respect to N for each E except for $E \geq 100$ is recorded in Table 4. As in Case I and Case II, it is clear that the tendency of velocity profile to oscillate is higher with E.

Downward trend of $Error\%_{av}$ with respect to E can be observed.

Table 4
Data corresponding to the time-step-based parameter, E and the number of mesh intervals, N after 400 time steps

E	N	Oscillation	*Error*	*Error%*	$Error\%_{av}$
1	20	NO	0	0	30.313
	40	NO	0.03356	6.712	
	80	NO	0.21597	43.205	
	160	NO	0.35669	71.337	
3.125	20	NO	0	0	15.374
	40	NO	0	0.001	
	80	NO	0.05812	11.626	
	160	NO	0.24934	49.867	
6.25	20	NO	0	0	8.096
	40	NO	0	0	
	80	NO	0.00828	1.657	
	160	NO	0.15364	30.727	
10	20	NO	0	0	4.346
	40	NO	0	0	
	80	NO	0.00072	0.143	
	160	NO	0.08621	17.241	
12.5	20	NO	0	0	2.936
	40	NO	0	0	
	80	NO	0.00009	0.018	
	160	NO	0.05863	11.726	
25	20	NO	0	0	0.435
	40	NO	0	0	
	80	NO	0.00009	0.017	
	160	NO	0.00860	1.721	
50	20	NO	0	0	0.015
	40	NO	0	0	
	80	NO	0.00009	0.017	
	160	NO	0.00022	0.044	
100	20	NO	0.00014	0.029	0.022
	40	NO	0.00007	0.015	
	80	NO	0.00011	0.022	
	160	NO	0.00012	0.023	

Even though there is no oscillation recorded in Table 4, upon closer analysis of $Error$ and $Error\%$, it is expected that the oscillation would occur for $E \geq 200$. This is due to an early sign of oscillation when $E = 100$ where there is a fluctuation in both $Error$ and $Error\%$.

3.2.4 Pattern of errors

Referring to Figure 3, in general, $Error\%$ decreases with the number of time steps when N is fixed, and increases with N when the number of time steps is constant.

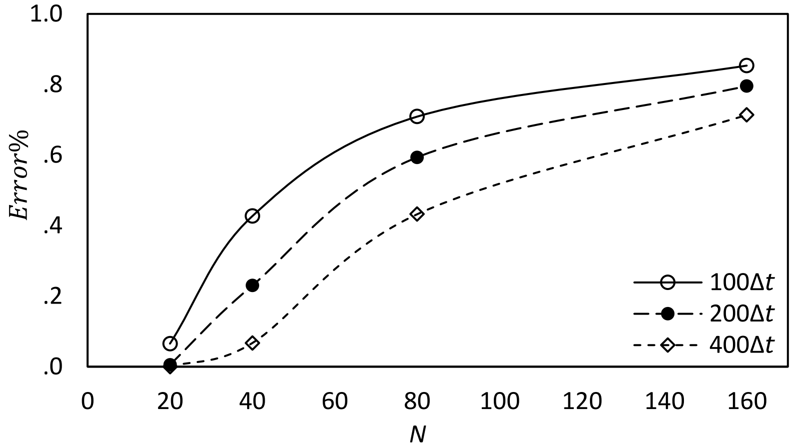

Fig. 3. Error percentage, $Error\%$ against the number of intervals, N for $E = 1$

As shown in Figure 4, $Error\%_{av}$ decreases with the number of time steps when E is constant, and decreases with E when the number of time steps is fixed. Note that these findings are specific to the unsteady Couette solution.

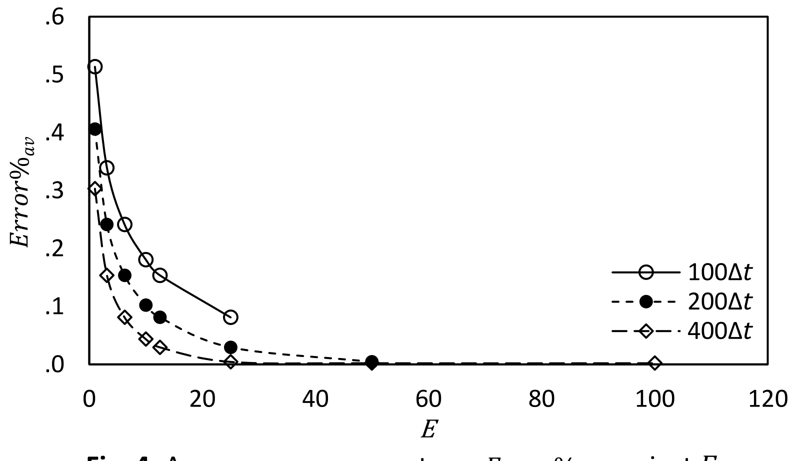

Fig. 4. Average error percentage, $Error\%_{av}$ against E

The specific equations, Eq. (10) and Eq. (11), demonstrate that when the value of N increases while E remains constant, both Δy^* and Δt^* decrease. This means that as the number of time steps increases, the error in the solution decreases, and the time interval between each step also decreases. However, it is important to note that a smaller Δt^* requires more time steps to reach a steady-state solution. Consequently, when a fixed number of time steps is used, the error in the solution tends to be larger as N increases. Furthermore, if we increase the value of E for a given N, it necessitates a greater Δt^*. This, in turn, leads to oscillation.

Additionally, the study found that increasing E can lead to a decrease in the average error percentage, $Error\%_{av}$ for all three cases of interest (*i.e.* those of 100, 200, and 400 time steps). However, this is not always the case for relatively large values of E, as the solution may start to oscillate. A careful analysis revealed a threshold value of E beyond which oscillation can be predicted. For example, in the case of 400 time steps, there is a slight chance of oscillation occurring for $E \geq 200$, as indicated by early signs when $E = 100$.

The error patterns observed in these simulations provide valuable information that can be leveraged in real applications to enhance the accuracy, efficiency, and reliability of computational simulations. By incorporating these findings into their workflow, engineers and researchers can improve the quality of their results, make informed decisions, and advance the state-of-the-art in their respective fields.

4. Conclusions

In conclusion, the error patterns identified in the simulations offer significant insights that can be effectively applied in practical scenarios to enhance the precision, effectiveness, and dependability of computational simulations. By integrating these observations into their practices, engineers and researchers have the opportunity to elevate the quality of their outcomes, make well-founded decisions, and propel advancements in their respective domains.

The study indicates that the error associated with the unsteady Couette solution escalates with an increase in the number of intervals, N. Nonetheless, augmenting the time-step-based parameter, E has the potential to mitigate the error, albeit with a concurrent rise in the probability of oscillation.

These results underscore the critical importance of taking into account the specific attributes of the problem under consideration when interpreting outcomes, particularly in cases involving unsteady solutions. The research underscores the necessity for a meticulous examination and comprehension of the parameters involved to precisely forecast the system's behavior.

Acknowledgement
This research was supported by Universiti Tun Hussein Onn Malaysia (UTHM) through Tier 1 (vot Q115).

References
[1] Rihan, Y. "Computational study of Couette flow between parallel plates for steady and unsteady cases." (2008).
[2] SKF, "Plain Bearings." https://www.skf.com/group/products/plain-bearings (accessed Jan. 26, 2023).
[3] Jiménez, Javier, Genta Kawahara, Mark P. Simens, Masato Nagata, and Makoto Shiba. "Characterization of near-wall turbulence in terms of equilibrium and "bursting" solutions." *Physics of Fluids* 17, no. 1 (2005). https://doi.org/10.1063/1.1825451
[4] Orlandi, Paolo, Matteo Bernardini, and Sergio Pirozzoli. "Poiseuille and Couette flows in the transitional and fully turbulent regime." *Journal of Fluid Mechanics* 770 (2015): 424-441. https://doi.org/10.1017/jfm.2015.138
[5] Hu, Sean, and Xiaolin Zhong. "Linear stability of viscous supersonic plane Couette flow." *Physics of Fluids* 10, no. 3 (1998): 709-729. https://doi.org/10.1063/1.869596
[6] Sukanek, Peter C., Charles A. Goldstein, and Robert L. Laurence. "The stability of plane Couette flow with viscous heating." *Journal of Fluid Mechanics* 57, no. 4 (1973): 651-670. https://doi.org/10.1017/S002211207300193X
[7] Tuckerman, Laurette S., Matthew Chantry, and Dwight Barkley. "Patterns in wall-bounded shear flows." *Annual Review of Fluid Mechanics* 52 (2020): 343-367. https://doi.org/10.1146/annurev-fluid-010719-060221
[8] Islam, S., Rehan Ali Shah, Ishtiaq Ali, and Nasro Min Allah. "Optimal homotopy asymptotic solutions of Couette and Poiseuille flows of a third grade fluid with heat transfer analysis." *International Journal of Nonlinear Sciences and Numerical Simulation* 11, no. 6 (2010): 389-400. https://doi.org/10.1515/IJNSNS.2010.11.6.389

[9] Domaradzki, J. Andrzej, and Ralph W. Metcalfe. "Direct numerical simulations of the effects of shear on turbulent Rayleigh-Bénard convection." *Journal of Fluid Mechanics* 193 (1988): 499-531. https://doi.org/10.1017/S002211208800223X

[10] Sukhtayev, Alim, Kevin Zumbrun, Soyeun Jung, and Raghavendra Venkatraman. "Diffusive stability of spatially periodic solutions of the Brusselator model." *Communications in Mathematical Physics* 358 (2018): 1-43. https://doi.org/10.1007/s00220-017-3056-x

[11] Dawson, Clint N., Qiang Du, and Todd F. Dupont. "A finite difference domain decomposition algorithm for numerical solution of the heat equation." *Mathematics of computation* 57, no. 195 (1991): 63-71. https://doi.org/10.2307/2938663

[12] Kuznik, Frédéric, and Joseph Virgone. "Experimental investigation of wallboard containing phase change material: Data for validation of numerical modeling." *Energy and Buildings* 41, no. 5 (2009): 561-570. https://doi.org/10.1016/j.enbuild.2008.11.022

[13] Olshanskii, Maxim A., Arnold Reusken, and Xianmin Xu. "An Eulerian space-time finite element method for diffusion problems on evolving surfaces." *SIAM journal on numerical analysis* 52, no. 3 (2014): 1354-1377. https://doi.org/10.1137/130918149

[14] Lord, Gabriel J., and Antoine Tambue. "A modified semi–implicit Euler–Maruyama scheme for finite element discretization of SPDEs with additive noise." *Applied Mathematics and Computation* 332 (2018): 105-122. https://doi.org/10.1016/j.amc.2018.03.014

[15] Liu, Shean-Lin. "Stable explicit difference approximations to parabolic partial differential equations." *AIChE Journal* 15, no. 3 (1969): 334-338. https://doi.org/10.1002/aic.690150308

[16] He, Yinnian, and Weiwei Sun. "Stability and convergence of the Crank–Nicolson/Adams–Bashforth scheme for the time-dependent Navier–Stokes equations." *SIAM Journal on Numerical Analysis* 45, no. 2 (2007): 837-869. https://doi.org/10.1137/050639910

[17] McCabe, Maurice, Peter K. Stansby, Benedict D. Rogers, and Lee S. Cunningham. "Boussinesq modelling of tsunami and storm wave impact." *Proceedings of the Institution of Civil Engineers-Engineering and Computational Mechanics* 167, no. 3 (2014): 106-116. https://doi.org/10.1680/eacm.13.00025

[18] A. Sharhan and A. H. Al-Muslimawi. "Numerical Study of Shear and Extensional Inelastic Contraction Flows." *CFD Letters* 15, no. 8 (2023): 107–121. https://doi.org/10.37934/cfdl.15.8.107121

[19] H. Hanafi, H. Hanif, S. Shafie, F. Bosli, and M. R. Ilias. "Unsteady Free Convection Dusty MHD Flow with Dissipation Effect Over Non-Isothermal Vertical Cone." *Journal of Advanced Research in Fluid Mechanics and Thermal Sciences* 114, no. 1 (2024): 56–68. https://doi.org/10.37934/arfmts.114.1.5668

[20] Khan, Amin, Muhammad Ahsan, Ebenezer Bonyah, Rashid Jan, Muhammad Nisar, Abdel-Haleem Abdel-Aty, and Ibrahim S. Yahia. "Numerical solution of Schrödinger equation by Crank–Nicolson method." *Mathematical Problems in Engineering* 2022 (2022). https://doi.org/10.1155/2022/6991067

[21] Jabbar, Ahmed. "The Finite Element Method for Nonlinear Huxely Equation." *University of Thi-Qar Journal of Science* 2, no. 2 (2010): 113-126.

[22] Zhao, Jie, Zhichao Fang, Hong Li, and Yang Liu. "A Crank–Nicolson finite volume element method for time fractional Sobolev equations on triangular grids." *Mathematics* 8, no. 9 (2020): 1591. https://doi.org/10.3390/math8091591

[23] John, D., and J. R. Anderson. "Computational fluid dynamics: the basics with applications." *Mechanical engineering series* (1995): 261-262.